Ozonolysis of α-phellandrene – Part 2: Compositional analysis of the secondary organic aerosol highlights the role of stabilised Criegee intermediates

Felix A. Mackenzie-Rae[1], Helen J. Wallis[2], Andrew R. Rickard[2,3], Kelly Pereira[2], Sandra M. Saunders[1], Xinming Wang[4,5], Jacqueline F. Hamilton[2]

[1]School of Molecular Sciences, The University of Western Australia, Crawley WA 6009, Australia
[2]Wolfson Atmospheric Chemistry Laboratories, Department of Chemistry, University of York, York, YO10 5DD, UK
[3]National Centre for Atmospheric Science, University of York, York, YO10 5DD, UK
[4]State Key Laboratory of Organic Geochemistry and Guangdong Key Laboratory of Environmental Protection and Resources Utilization, Guangzhou Institute of Geochemistry, Chinese Academy of Sciences, Guangzhou 510640, China
[5]Center for Excellence in Regional Atmospheric Environment, Institute of Urban Environment, Chinese Academy of Sciences, Xiamen 361021, China

Correspondence to: J. Hamilton (jacqui.hamilton@york.ac.uk)

S.1 Tandem Mass Spectra

Tandem mass spectra for products identified using negative mode ESI, with fragment location sites shown by red lines.
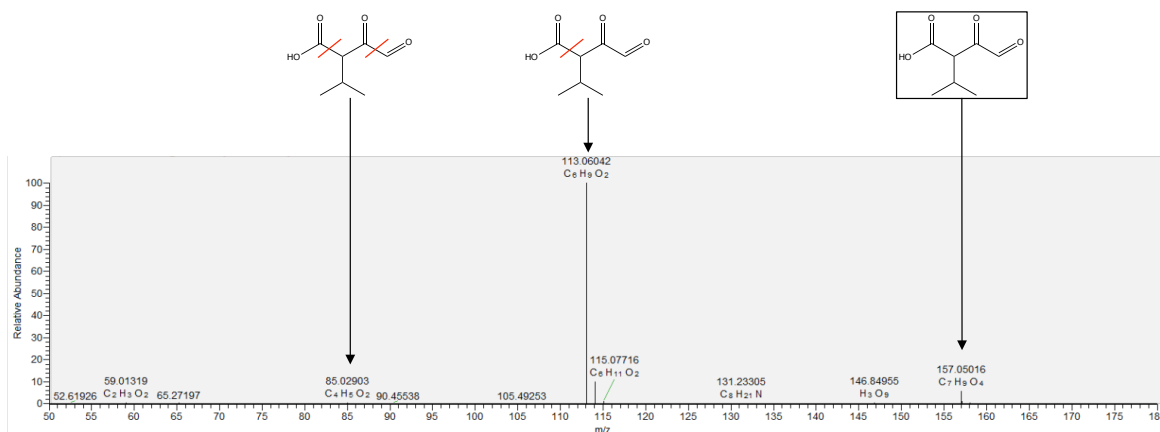

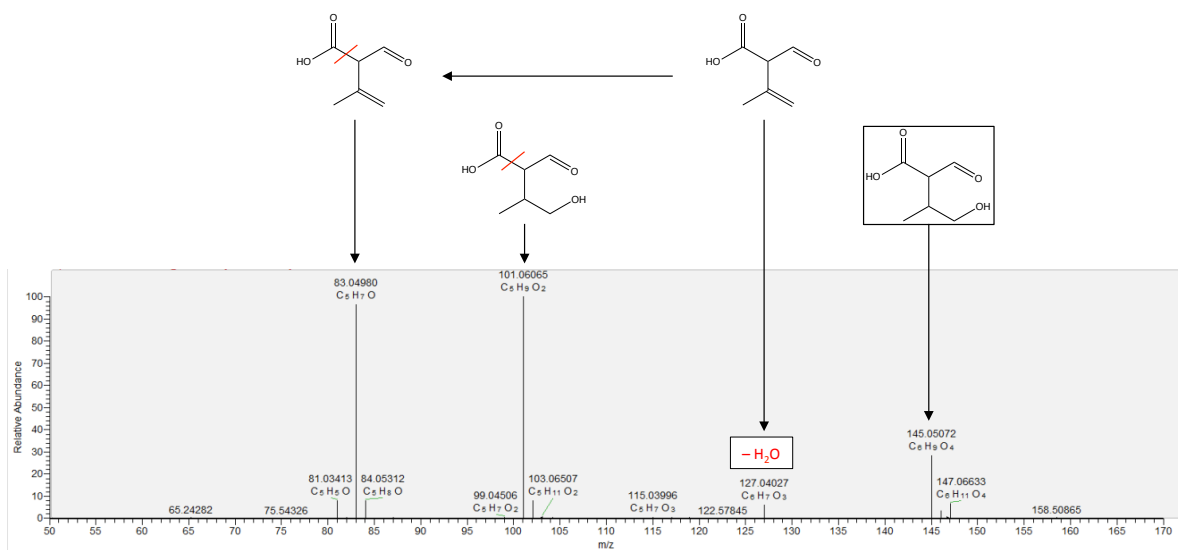**Figure S1.1: Tandem mass spectrum of compound N1.**
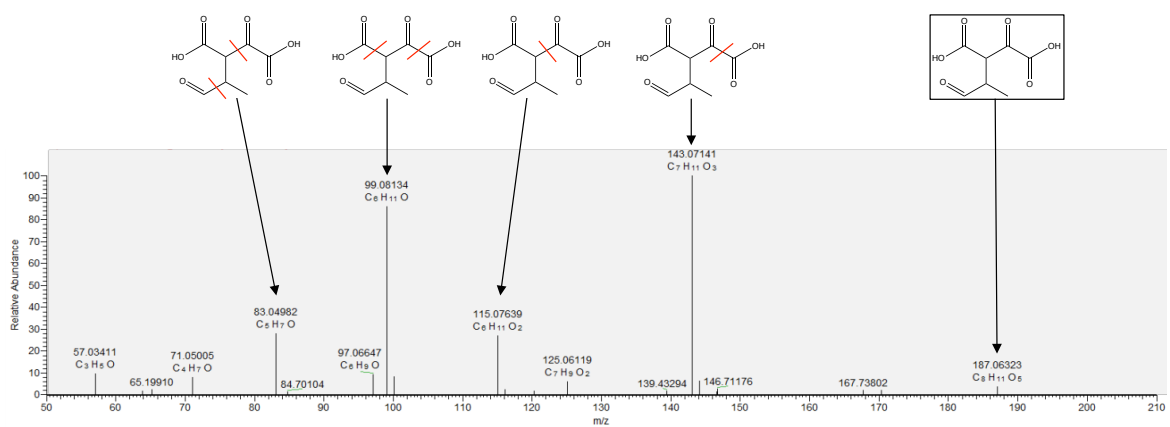
Figure S1.2: Tandem mass spectrum of compound N2.

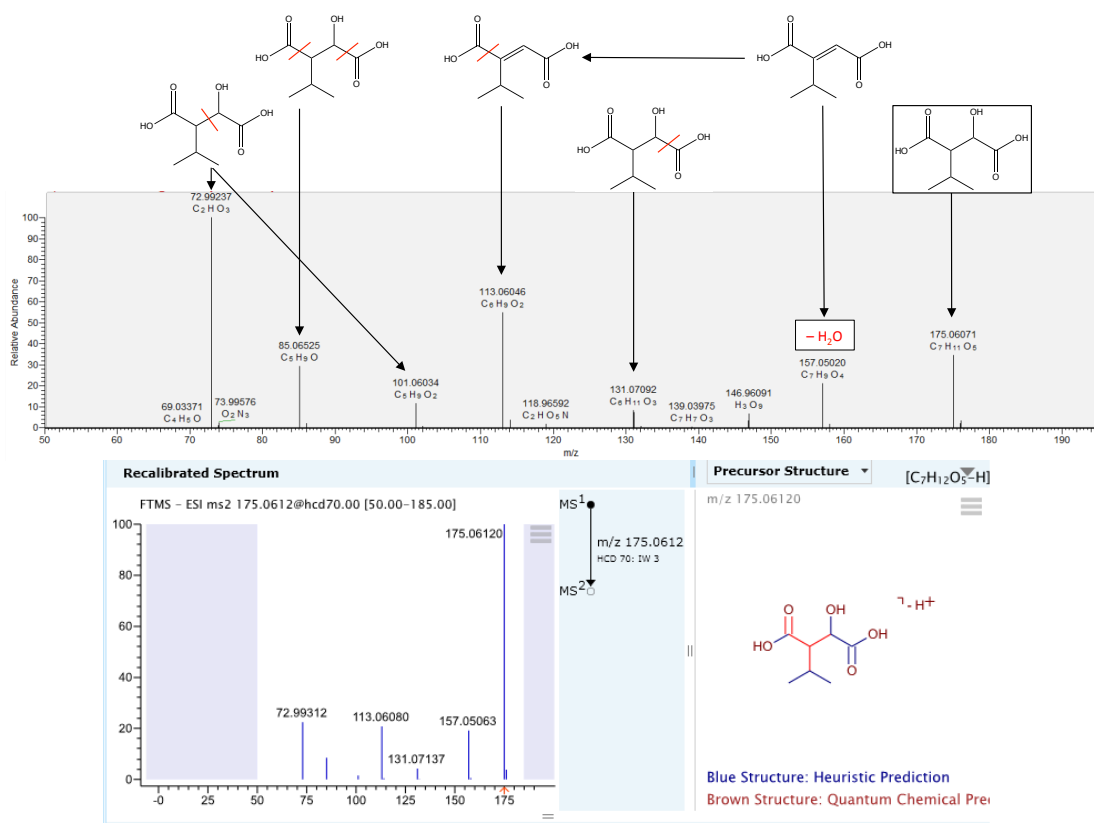**Figure S1.3: Tandem mass spectrum of compound N3.**

Figure S1.4: Tandem mass spectrum of compound N4 with mzcloud comparison.
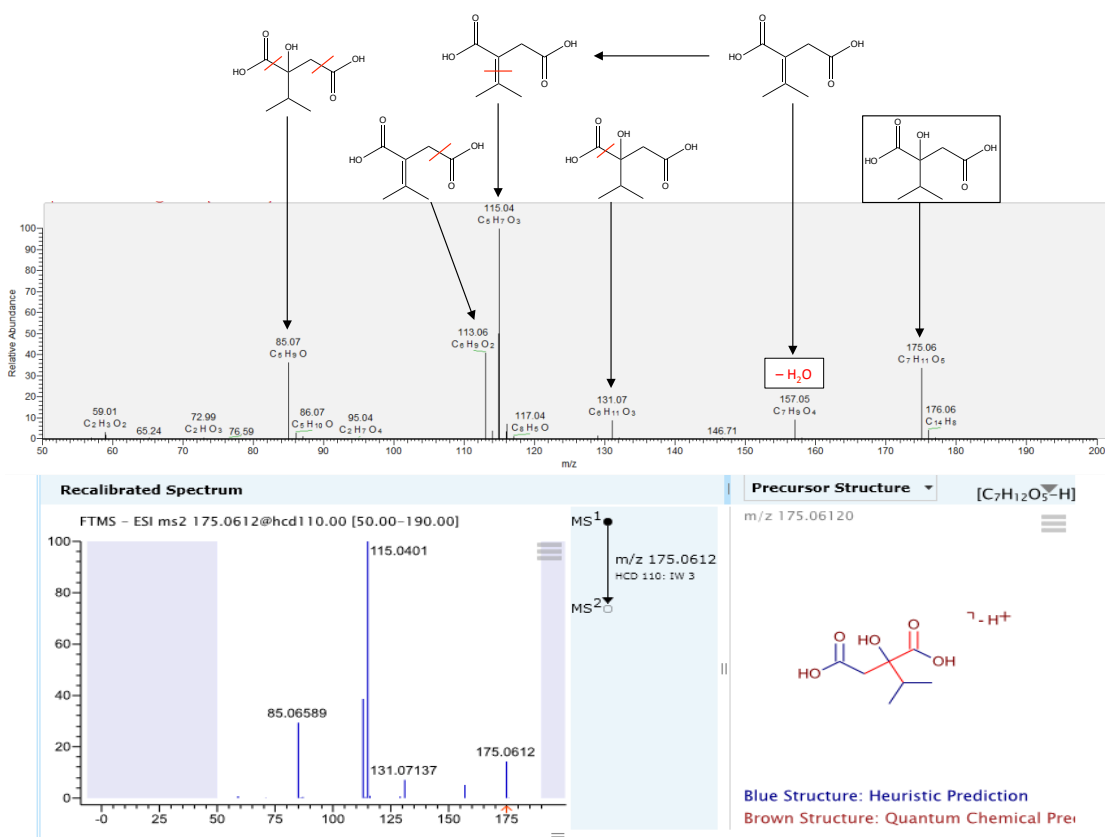

Figure S1.5: Tandem mass spectrum of compound N5 with mzcloud comparison.
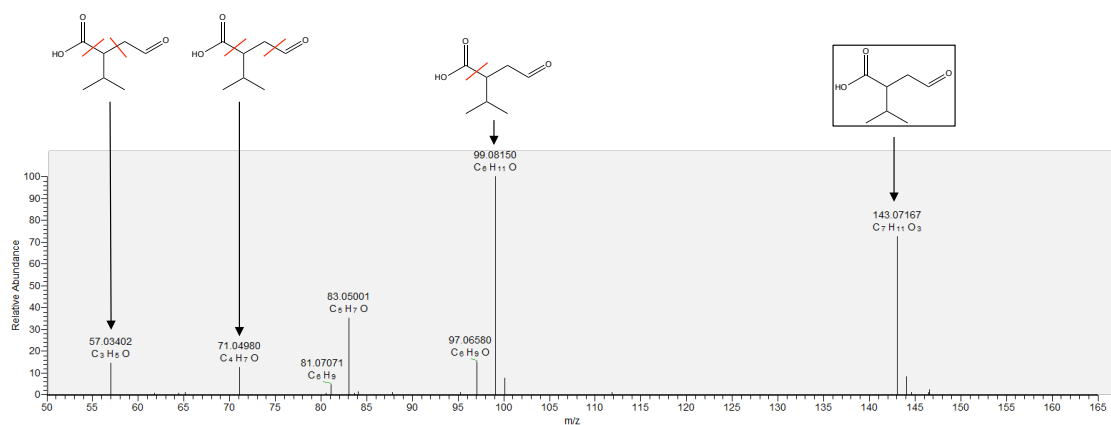
Figure S1.6: Tandem mass spectrum of compound N6.

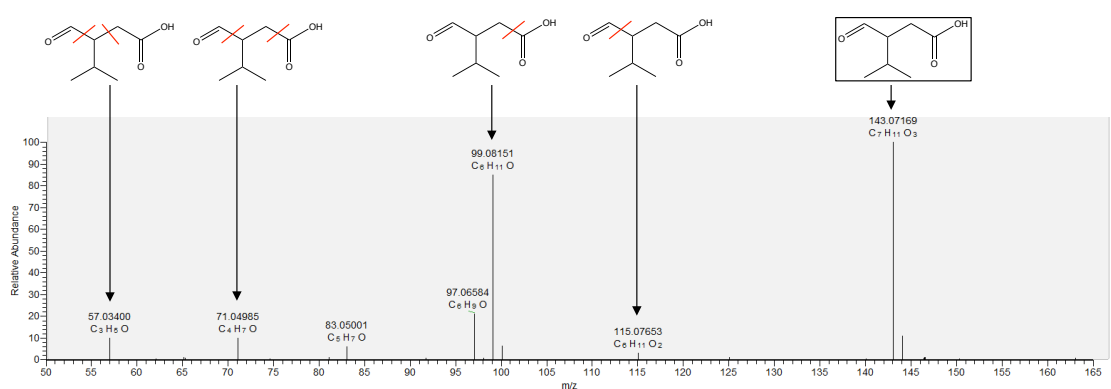**Figure S1.7: Tandem mass spectrum of compound N7.**
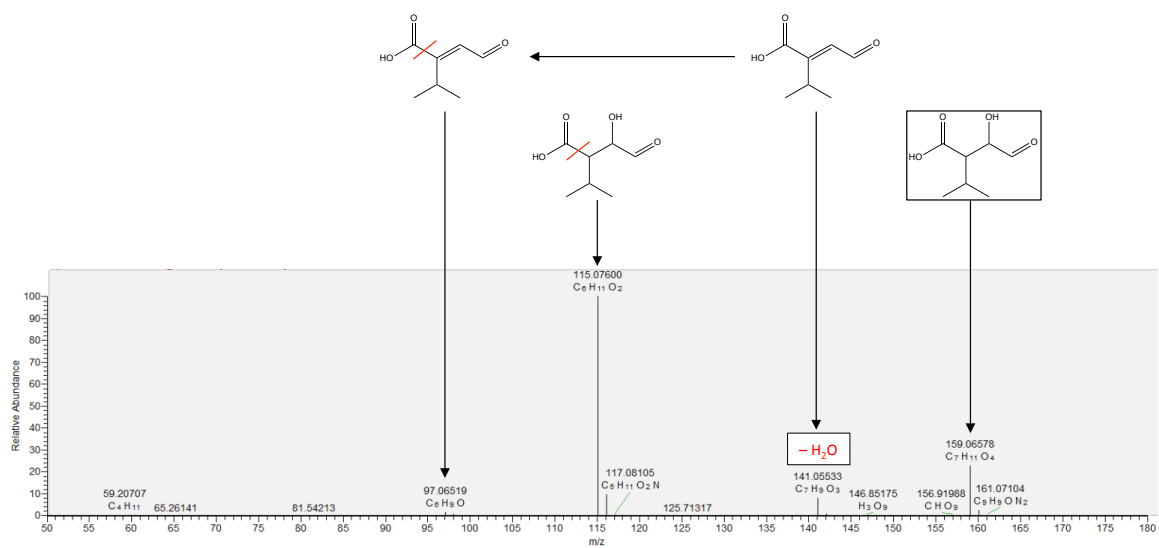

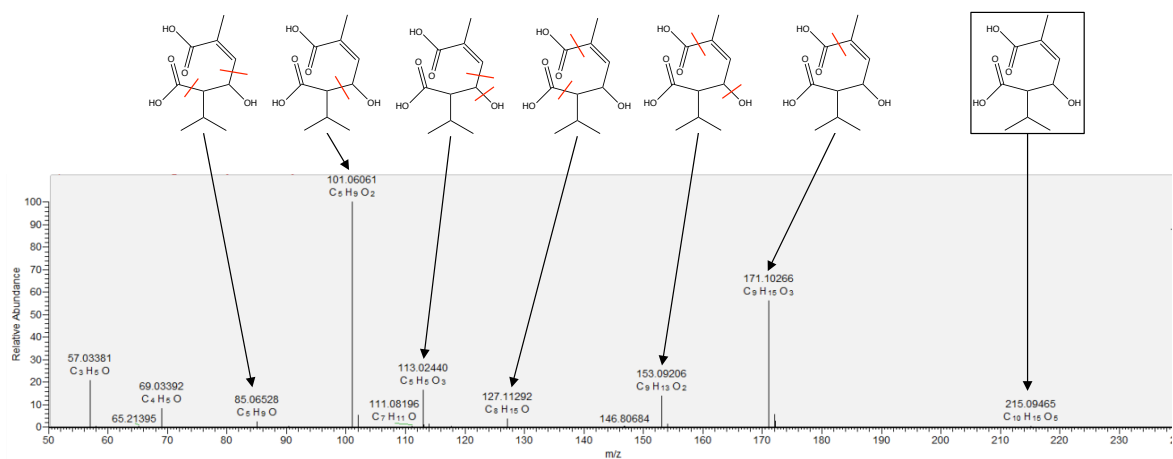**Figure S1.8: Tandem mass spectrum of compound N8.**

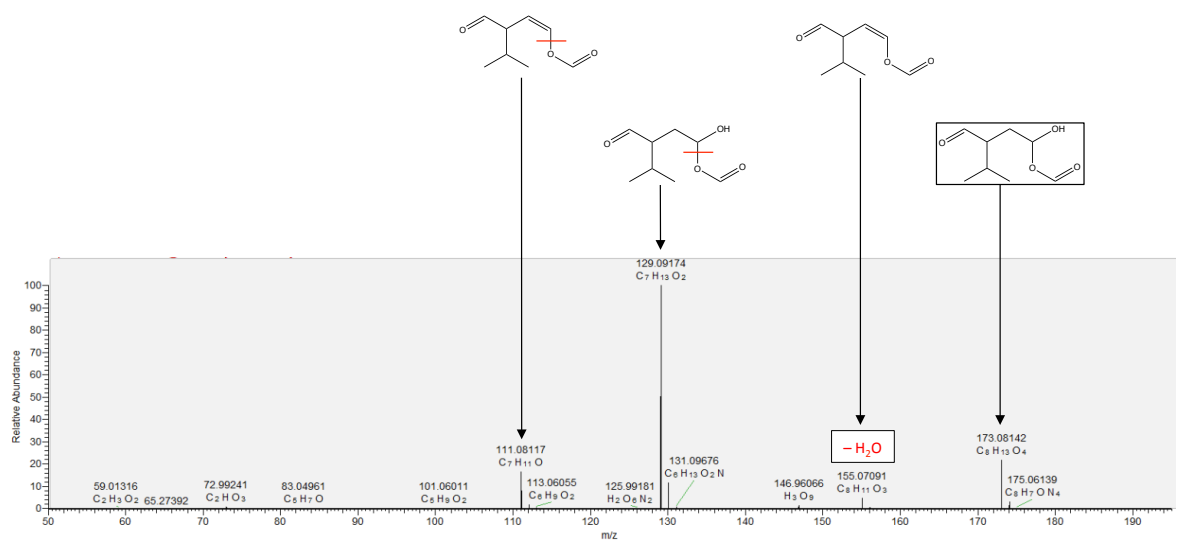**Figure S1.9: Tandem mass spectrum of compound N9.**

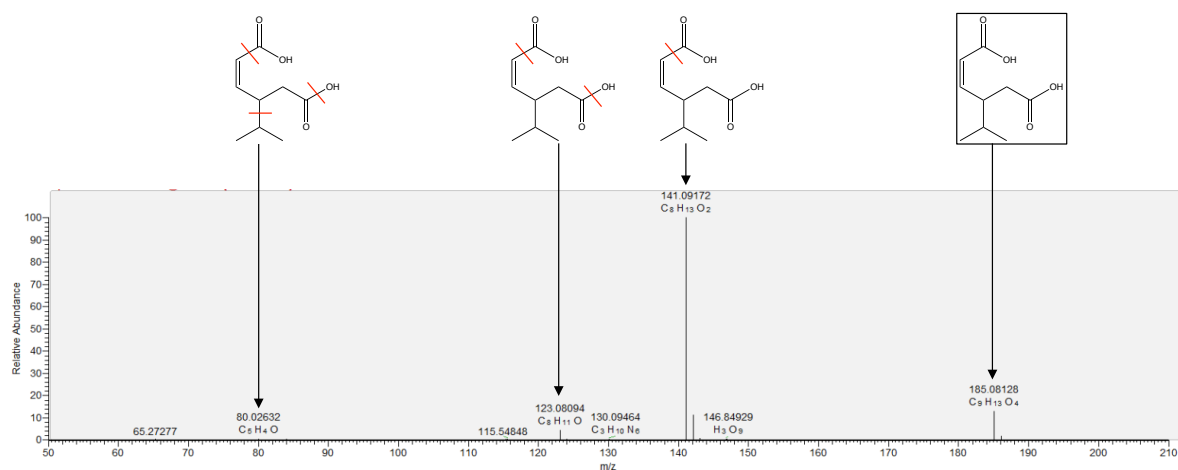**Figure S1.10: Tandem mass spectrum of compound N10.**

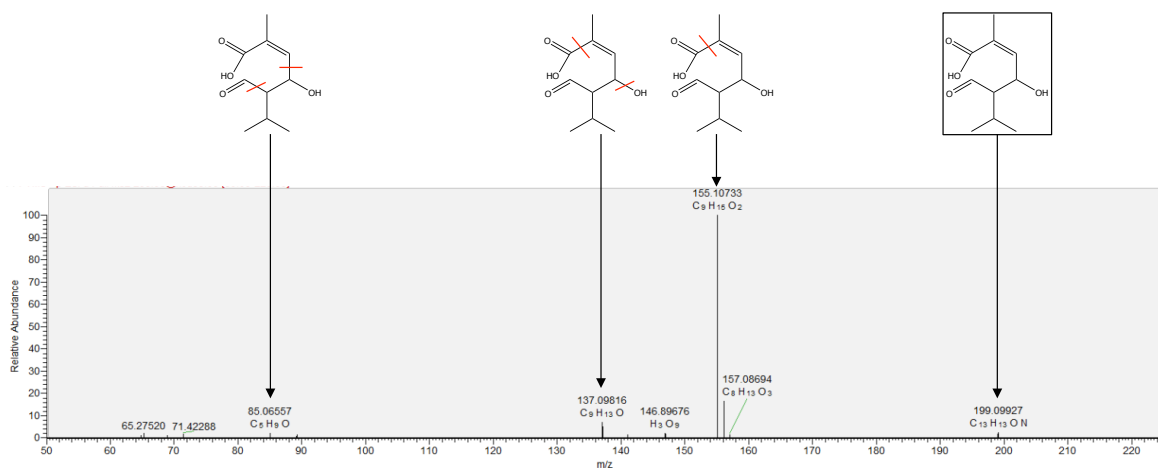**Figure S1.11: Tandem mass spectrum of compound N11.**

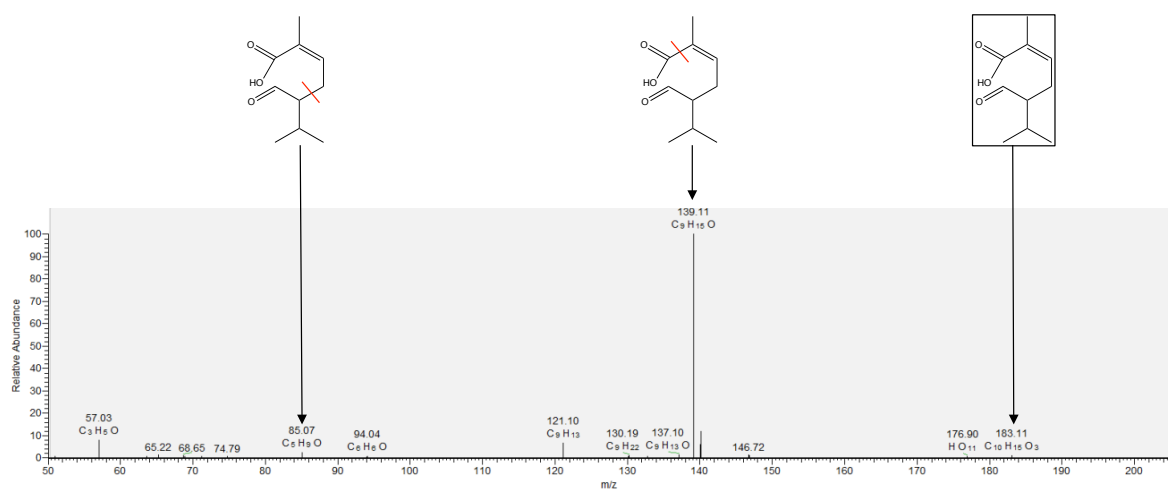**Figure S1.12: Tandem mass spectrum of compound N12.**

Figure S1.13: Tandem mass spectrum of compound N13.

S.2 Formation Mechanism of Compound N11

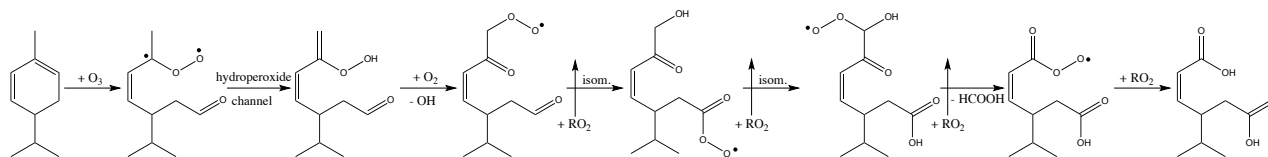The proposed formation mechanism of compound N11 is shown in Figure S.2 below.

Figure S2: Proposed pathway for formation of compound N11.

The pathway involves a vinyl hydroperoxide re-arrangement which has been shown by theoretical calculations to be uncompetitive with other pathways (Mackenzie-Rae et al., 2016). Additionally the mechanism utilises unconventional 1,8-acyl H-shifts, which occur through large, thermodynamically unfavourable cyclic intermediates. As a result the proposed structure and its formation mechanism remains tentative.

S.3 Saturation Vapour Concentration Estimation

The online molecular property predictor UManSysProp (Topping et al., 2016) was used to estimate both pure component vapour pressures and activities. Vapour pressures (P_L, Pa) were estimated using the structure based estimator of Nannoolal et al. (2004) for boiling points coupled with Nannoolal et al. (2008) for vapour pressures. This method has been extensively compared with other structural estimation techniques available in the literature with favourable results (Barley and McFiggans, 2010; O'Meara et al., 2014), although it is noted that it has performed poorly when representing multi-functional organic molecules that contain a high number of hydrogen bonding groups (≥ 4). Activity coefficients (γ) were calculated for a mixed organic system using Aerosol Inorganic-Organic Mixtures Functional groups Activity Coefficients (AIOMFAC, Zuend et al., 2008, 2011), and ranged from $0.46 < \gamma < 1.43$. Saturation vapour concentrations (C*, µg m^{-3}) were then calculated using these estimated parameters from the following formula (Donahue et al., 2006; Pankow, 1994):

$$C^* = \frac{10^6 MW_{om}\, \gamma\, P_L}{R\, T\, f_{om}}$$

where MW_{om} is the mean molecular weight of the condensed organic material (g mol^{-1}), R is the ideal gas constant (8.314 J K^{-1} mol^{-1}), T is the temperature (K) and f_{om} is the weight fraction of the particle phase that is absorbing organic material, which is taken as unity in this work.

S.4 Kendrick Mass Analysis

Using assigned chemical formulas for major spectral peaks (RI > 5%), a Kendrick mass analysis was performed by examining CH_2 and O mass defects. Essentially Kendrick plots aid in recognition of homologous families of molecules built by repeated addition of structural units, by re-normalising the IUPAC scale to a Kendrick scale (Kendrick, 1963). In this study, the Kendrick masses KM_{CH_2} and KM_O are calculated by normalising the exact masses of $^{12}CH_2$ to 14 amu and ^{16}O to 16 amu respectively. Kendrick mass defects (KMD) are then calculated as the difference between the nominal Kendrick mass

(rounded up to the nearest integer) and the actual Kendrick masses. Plotting the Kendrick mass defect against the Kendrick mass creates a Kendrick plot, as shown below.
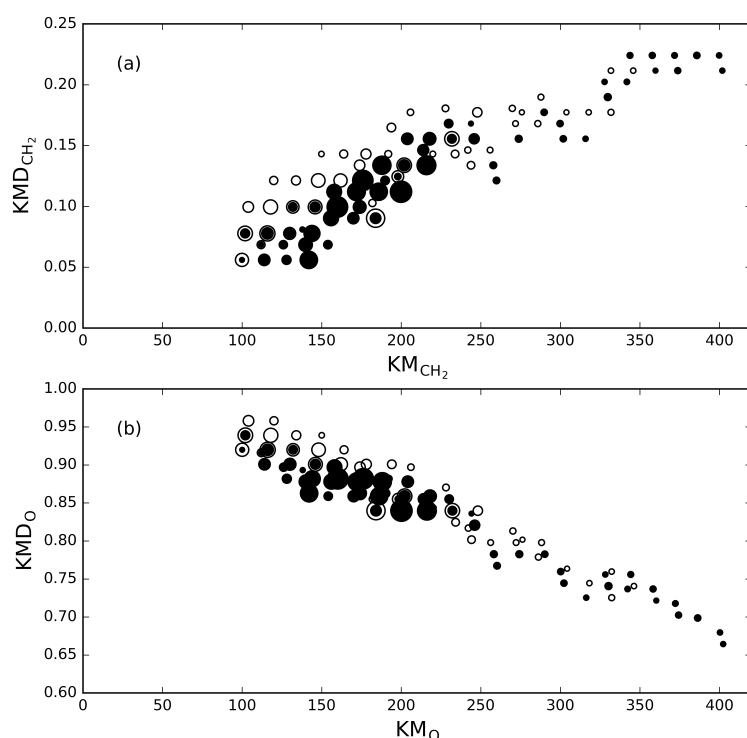

Figure S4: (a) CH$_2$ Kendrick plot and (b) O Kendrick plot for ions (RI > 5%) detected in the positive (open circles) and negative (closed circles) ionisation mode spectra. The size of the data point is proportional to relative signal intensity.

Figure S4a shows the CH$_2$ Kendrick mass plot constructed using data from both the positive and negative ionisation modes. Here species separated by CH$_2$ units fall on horizontal lines corresponding to families of the form C$_x$H$_y$O$_z$(CH$_2$)$_n$, where x, y and z are fixed and n is variable within a group. Overall, family groups contain on average 3 – 4 members with the largest containing 7, and show CH$_2$ is a common denomination between SOA constituents from α-phellandrene ozonolysis. Going towards heavier compounds there is a gradual increase in KMD_{CH_2}, which in general implies a higher degree of oxidation (Reinhardt et al., 2007; Walser et al., 2008), although there is a noticeable decrease in slope when transitioning from monomers to dimers.

Figure S4b shows the O Kendrick mass plot, in which horizontal lines now correspond to families of the form C$_x$H$_y$O$_z$, where x and y are fixed and z variable, that is families of species separated only by number of oxygen atoms. This time family groups averaged one member, indicating that CH$_2$ is a more common denominator than oxygen atoms between product species. This implies that fragmentation and/or accretion is more prominent in the system than functionalisation, although peaks resulting from fragmentation may skew results along with any biases in chemical formula assignment. Nonetheless numerous product families containing up to 5 species, e.g. C$_{10}$H$_{16}$O$_{3-7}$ or C$_7$H$_{12}$O$_{2-6}$, were observed, showing that radical re-arrangement and oxygen addition processes remain important.

References

Barley, M. H. and McFiggans, G.: The critical assessment of vapour pressure estimation methods for use in modelling the formation of atmospheric organic aerosol, Atmos. Chem. Phys., 10, 749–767, doi:10.5194/acp-10-749-2010, 2010.

Donahue, N. M., Robinson, A. L., Stanier, C. O. and Pandis, S. N.: Coupled partitioning, dilution, and chemical aging of semivolatile organics, Environ. Sci. Technol., 40, 2635–2643, doi:10.1021/es052297c, 2006.

Kendrick, E.: A Mass Scale Based on CH = 14.0000 for High Resolution Mass Spectrometry of Organic Compounds, Anal. Chem., 35(13), 2146–2154, doi:10.1021/ac60206a048, 1963.

Nannoolal, Y., Rarey, J., Ramjugernath, D. and Cordes, W.: Estimation of pure component properties: Part 1. Estimation of the normal boiling point of non-electrolyte organic compounds via group contributions and group interactions, Fluid Phase Equilib., 226, 45–63, doi:10.1016/j.fluid.2004.09.001, 2004.

Nannoolal, Y., Rarey, J. and Ramjugernath, D.: Estimation of pure component properties part 3. Estimation of the vapor pressure of non-electrolyte organic compounds via group contribution and group interactions, Fluid Phase Equilib., 269(1–2), 117–133, doi:10.1016/j.fluid.2008.04.020, 2008.

O'Meara, S., Booth, A. M., Barley, M. H., Topping, D. and McFiggans, G.: An assessment of vapour pressure estimation methods., Phys. Chem. Chem. Phys., 16(36), 19453–19469, doi:10.1039/c4cp00857j, 2014.

Pankow, J. F.: An absorption model of gas/particle partitioning of organic compounds in the atmosphere, Atmos. Environ., 28, 185–188, doi:10.1016/1352-2310(94)90093-0, 1994.

Reinhardt, A., Emmenegger, C., Gerrits, B., Panse, C., Dommen, J., Baltensperger, U., Zenobi, R. and Kalberer, M.: Ultrahigh mass resolution and accurate mass measurements as a tool to characterize oligomers in secondary organic aerosols, Anal. Chem., 79(11), 4074–4082, doi:10.1021/ac062425v, 2007.

Topping, D., Barley, M., Bane, M. K., Higham, N., Aumont, B., Dingle, N. and McFiggans, G.: UManSysProp v1.0: an online and open-source facility for molecular property prediction and atmospheric aerosol calculations, Geosci. Model Dev., 9(2), 899–914, doi:10.5194/gmd-9-899-2016, 2016.

Walser, M. L., Desyaterik, Y., Laskin, J., Laskin, A. and Nizkorodov, S. A.: High-resolution mass spectrometric analysis of secondary organic aerosol produced by ozonation of limonene., Phys. Chem. Chem. Phys., 10, 1009–1022, doi:10.1039/B712620D, 2008.

Zuend, A., Marcolli, C., Luo, B. P. and Peter, T.: A thermodynamic model of mixed organic-inorganic aerosols to predict activity coefficients, Atmos. Chem. Phys., 8, 4559–4593, doi:10.5194/acpd-8-6069-2008, 2008.

Zuend, A., Marcolli, C., Booth, A. M., Lienhard, D. M., Soonsin, V., Krieger, U. K., Topping, D. O., McFiggans, G., Peter, T. and Seinfeld, J. H.: New and extended parameterization of the thermodynamic model AIOMFAC: calculation of activity coefficients for organic-inorganic mixtures containing carboxyl, hydroxyl, carbonyl, ether, ester, alkenyl, alkyl, and aromatic functional groups, Atmos. Chem. Phys., 11(17), 9155–9206, doi:10.5194/acp-11-9155-2011, 2011.